Test Evaluation and Computational Modeling Applicability for Compression Moldability of Inert Explosive

Jin Sung Lee and Jung Su Park
Agency for Defense Development, Yuseong P.O. Box 35-4, Daejeon, South Korea

Keywords: Shima-Oyane Yield Model, Powder, Moldability Behaviour, Double Action Pressing, Isostatic Pressing, Computational Model Analysis.

Abstract: Using an inert explosive powder, molding experiments were carried out. And a computational model analysis was performed to predict moldability behaviour of an inert explosive powder. In order to analysis the Shima-Oyane yield model to predict the behaviour of the densification for inert explosive powder, using an inert explosive powder was carried out moldability tests on the pressure, could be obtained volumetric strain on the pressure, relative density and so on. Based on the results of the curve fitting, it could be derived the parameters for the yield function of the cap with the critical state. Finite element analysis for both double action pressing and isostatic pressing process of the two yield models were performed. And changes in relative density and densification behaviour of an inert explosive powder were analysed. In addition, it investigated the distribution of the relative density or volumetric strain caused by the overall and local variations. It was founded the maximum stress and position etc. under working pressure of inert explosive powder.

1 INTRODUCTION

In the manufacturing technologies of P/M products, isostatic pressing and die compression are widely used. However, P/M parts formed by die compression have inhomogeneous density distributions due to the friction between the powder and die wall.

Process simulations by using a finite element analysis may be useful to control the shape during P/M forming process (Lewis, 1993), (Gethin, 1994). The numerical modelling of the powder compression process requires the appreciate constitutive models for densification of a powder material. A number of yield functions have been developed for densification behaviour of powder material, so far.

By including the effect of hydrostatic stress on plastic deformations of porous materials (Kuhn and Downey, 1971), (Shima-Oyane, 1976), and (Doraivelu et al., 1984) proposed yield functions from uniaxial tests of powder compressions. (Fleck et al.,1992) proposed a microscopic constitutive model from particle deformations. The yield function by Fleck et al., however, did not agree well with experimental data of soft metal powder during die compaction (Kwon, 1997). A number of researchers also adopted models for densification of powder from soil mechanics. Watson et al., (1993) investigated yield criteria of powder by using the Drucker-Prager-/Cap model.

In this paper, using an inert explosive powder as a soft powder material, molding experiments were carried out. And a computational model analysis was performed to predict moldability behaviour of an inert explosive powder.

To apply Shima-Oyane, Drucker-Prager/Cap yield model to predict the behaviour of the densification for inert explosive powder, using an inert explosive powder were carried out moldability tests. Finite element analysis for double action pressing and isostatic pressing process were performed.

2 ANALYSIS

2.1 Constitutive Model

In die compression, the deformation behaviour of the powder body is based on the yield criterion. Unlike bulk solids, the yield criterion includes the hydrostatic pressure due to volume change in compression. Among many yield criteria for

Lee, J. and Park, J.
Test Evaluation and Computational Modeling Applicability for Compression Moldability of Inert Explosive.
DOI: 10.5220/0006832504290434
In *Proceedings of 8th International Conference on Simulation and Modeling Methodologies, Technologies and Applications (SIMULTECH 2018)*, pages 429-434
ISBN: 978-989-758-323-0

compression, Shima-Oyane's criteria is of the generalized form

$$\Phi = \left(\frac{q}{\sigma_m}\right)^2 + c(1-\rho)^\gamma \left(\frac{p}{\sigma_m}\right)^2 - \rho^m \qquad (1)$$

Where, q and p are the effective stress and hydrostatic pressure, ρ is relative density σ_m is the flow stress of matrix material. c, γ and m are the material parameters.

The complicated procedure to determine the material parameters including the flow stress of matrix material σ_m and the friction coefficient μ has obstructed the practical use of the numerical simulation in the process. In this paper, we tried to find the material parameters, from the die compression test. We assumed the following expression for the flow stress of matrix material σ_m:

$$\sigma_m = a + b\bar{\varepsilon}_m^n \qquad (2)$$

Where, a, b, and n are the material parameters and ε_m is the effective strain of matrix material.

2.2 Damage Model

In die compression process, crack formulation during compression and ejection is very important problem. In this paper, we used Shima-Oyane yield model and Drucker-Prager failure surface for the crack formulation. Shima-Oyane model is elliptical shape in the stress space as shown figure 1.

A new concept for crack formulation, failure separation length(FSL), can be considered. FSL means the accumulated separation length from Drucker-Prager failure surface as shown in figure 1.

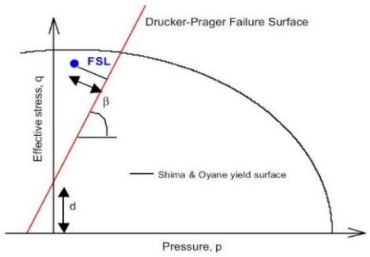

**FSL : Failure Separation Length

Figure 1: Shima-Oyane yield surface and Drucker-Prager failure surface.

During the numerical simulation of die compression process, we can investigate the stress path of all elements and we can check whether a specific region go over the Drucker-Prager failure surface. The accumulated separation length from Drucker-Prager failure surface can show the possibility of crack formulation.

Finite element calculations were obtained by using Shima-Oyane model in the constitutive library provide in PMsolver S/W.

3 EXPERIMENTS

3.1 Test Equipment

Figure 2: Hydraulic press.

Figure 3: Isostatic press.

The test equipment for this study are double action hydraulic press and isostatic press. Double action press in figure 2 was used to test the pressing of a cylindrical shaped body to compare with the results of computational analysis, the compression moldability evaluation test to check the density against various pressures, and the friction coefficient.

Isostatic press in figure 3 was used to make shaped body for comparison with computational analysis results.

3.2 Determination of Material Parameters

Compression moldability is evaluated by using inert

explosive and a suitable compression molding simulation model is presented. The composition used for the test was compression molded at room temperature as shown in table 1.

Table 1: Inert explosive composition.

No.	Composition(wt.%)	TMD (g/cm^3)
1	$CaCO_3$/Pentaerythritol/$(NH_4)_2SO_4$/Binder system = 22/6/64/8	1.746

** TMD: Theoretical Maximum Density(g/cm^3)

Die compression response of inert explosive powder was investigated in a closed die under double action pressing. The inert explosive powder was pressed under axial pressure from 4.74 to 173 MPa as shown in figure 4.

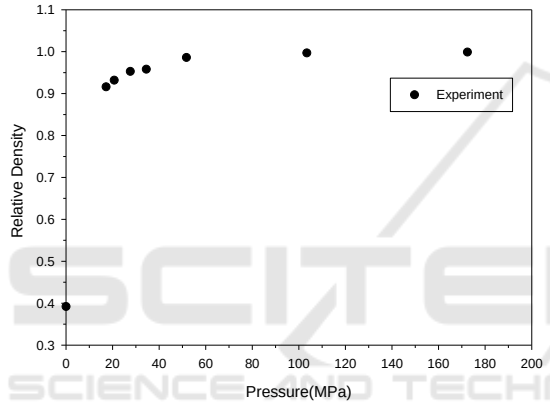

Figure 4: Variation of relative density with pressure of inert explosive powder for various pressures (TMD = 1.746 g/cm^3).

In this work, we used the same material parameters c and γ that Shima-Oyane used for the iron based powder as follows:

$$c = 6.20,\ \gamma = 1.028 \quad (3)$$

The material parameter m and the flow stress of matrix material σ_m were obtained by minimizing the difference between the calculation and the measured variation of relative density with pressure during the die compression process without friction effect. The material parameter m and the flow stress of matrix material were determined as follows:

m = 4.1109

$$\sigma_m = a + b\bar{\varepsilon}_m^n \quad (4)$$

Where, a = 14.1248, b = 0.0001, and n = 11.358

Die compression tests were performed with two different methods to get the pressure-density response of the inert explosive powder without and with friction effect as shown in figure 5.

To investigate the relation between the relative density and pressure of the inert explosive powder without the friction effect, silicone type lubricant was applied on the die wall and small amount of powder(15g) was poured in a closed with 36 mm in diameter. The big amount(45g) of inert explosive powder used to test friction effect.

It was found that specimen(15g) had a slightly higher density than specimen(47g) in the low pressure region, and the density difference between the two specimens disappeared with increasing pressure. At the final pressure of 173 MPa, the relative density of the two specimens was 0.99, which was the same value.

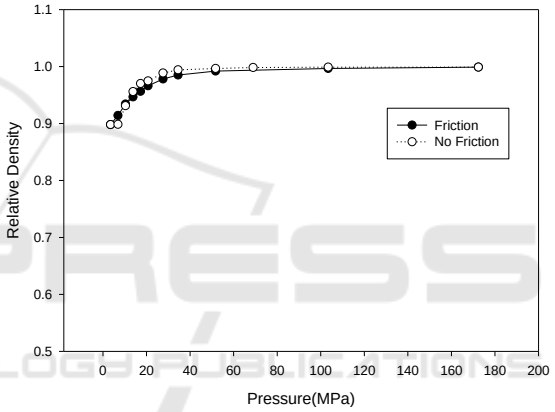

Figure 5: Variation of relative density with pressure of inert explosive powder under frictional condition during double action pressing.

Figure 6 shows variation of relative density with pressure of inert explosive during die compression. The friction coefficient between the inert explosive powder and the mold was varied through computational analysis to obtain the friction coefficient with the pressure and relative density curve shown in the experiment.

The friction coefficient $\mu = 0.2$ was obtained by minimizing the difference between the finite element simulation results with the determined material parameters in Eqs. (3) and (4) and the measured variation of relative density with pressure during the die compression process with friction.

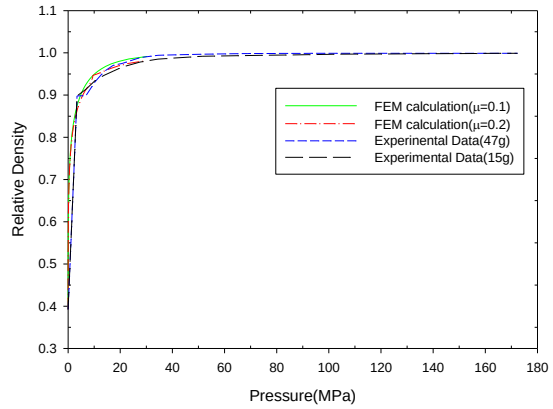

Figure 6: Variation of relative density with pressure of inert explosive during die compression.

In this study, a uniaxial test was carried out using a 36 mm diameter pellet. Figure 7 shows a stress-strain curve of the inert explosive pellet. Table 2 shows mechanical properties of inert explosive pellet.

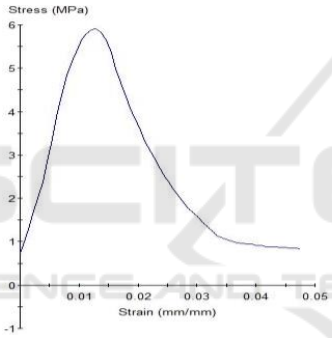

Figure 7: Stress-strain curve of the inert explosive.

Table 2: Mechanical properties.

Yield Strength (MPa)	Young's Modulus (MPa)	Poisson's ratio	Shear Modulus (MPa)
5.87	608.97	0.272	239.37

4 RESULTS AND DISCUSSION

4.1 Double Action Pressing Model

Figure 8 shows the double action pressing model. The analytical model uses a 36.09 mm diameter cylindrical mold and compresses the inert explosive powder by compressing both sides at the same time.

As a results of double action pressing for inert explosive powder in table 3, the final shape was almost identical when comparing the test results and the analysis results. The difference between the initial height of the test results and the analysis results in the table 3 is the difference in applying the method to reduce the mesh errors in the analysis.

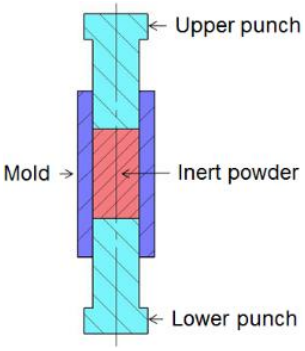

Figure 8: Double action pressing model: Schematic drawing of the mold.

Table 3: Results of inert explosive pellet.

	Experiment	Simulation
Weight(g)	63.65	63.65
Initial diameter(mm)	36.09	36.09
Initial height(mm)	90.83	49.32
Initial density(g/cm^3)	0.685	1.262
After pressing diameter(mm)	36.04	36.09
After pressing height(mm)	35.78	35.85
After pressing density(g/cm^3)	1.744	1.736

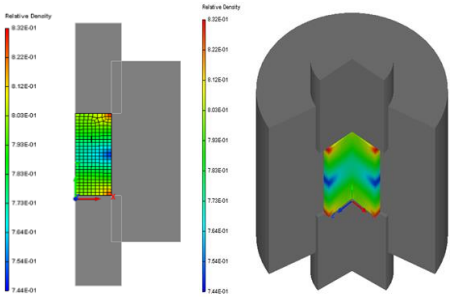

Figure 9: Double action pressing process with relative density 0.74–0.83.

Figure 9 shows the range of relative density 0.74-0.83 in the progress of compression, showing the characteristic of double action pressing in which the density of the end part of the shaped body is higher

and the density of the intermediate part of the shaped body is lower.

Figure 10 shows the state over the range of relative density 0.99 in the progress of compression and shows that the shaped body has a uniform density distribution as a whole.

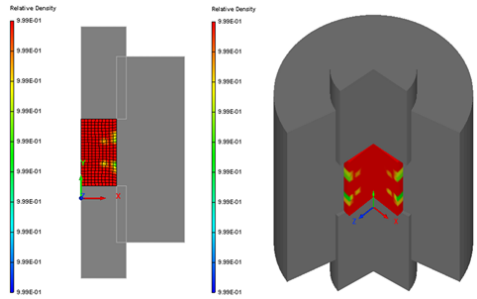

Figure 10: Double action pressing process with relative density 0.99 over.

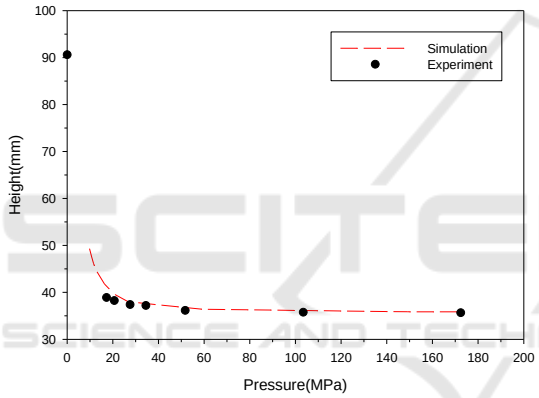

Figure 11: Variation of pellet height with pressure during die compression of Shima-Oyane yield model.

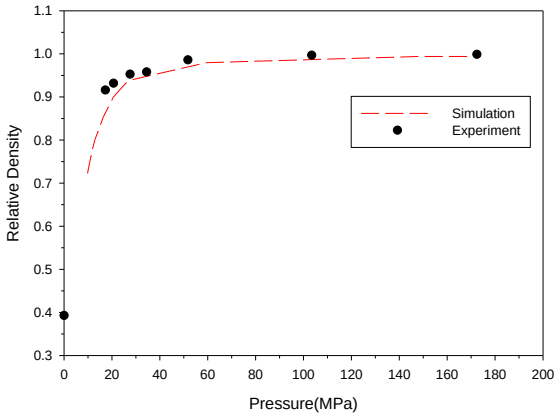

Figure 12: Variation of relative density with pressure during die compression of Shima-Oyane yield model.

Figure 11 shows variation of pellet height with pressure during die compression of Shima-Oyane yield model. It can be seen that the height difference of the shaped body is relative large in the low pressure range of the test process and analysis process, and the difference is small as it goes the height pressure range.

Figure 12 shows variation of relative density with pressure during die compression of Shima-Oyane yield model. As the compressive pressure increase, the maximum relative density approaches 1.

4.2 Isostatic Pressing Model

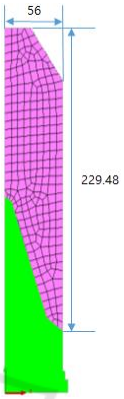

Figure 13: Isostatic pressing modeling of Shima-Oyane yield model.

Figure 13 shows isostatic pressing modeling of Shima-Oyane yield model. Axisymmetric modelling was carried out based on tests using mold of shaped charge type with a diameter of 112 mm.

Figure 14 shows results of inert explosive pressing simulation about pressing states with relative densities. Figure 14(b) shows density concentration or stress concentration at the top of the mold in the progress of compression. When changing the shape of a mold in a similar shape, it is necessary to consider the design of the mold because the concentrated stress may appear at that part.

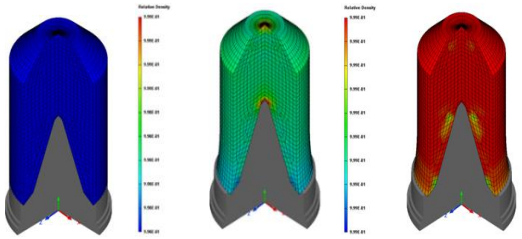

(a) (b) (c)

Figure 14: Results of inert explosive pressing simulation : (a) Before pressing with relative density 0.573 ; (b) Pressing with relative density 0.98 – 0.99; (c) After pressing with relative density 0.99 over.

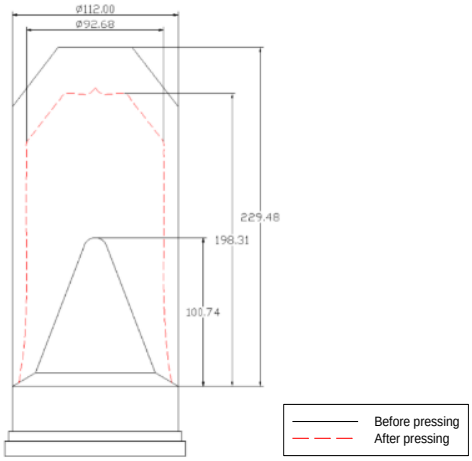

Figure 15: Result of isostatic pressing simulation with Shima-Oyane yield model.

Figure 15 shows result of isostatic pressing simulation with Shima-Oyane yield model. The black line is the shape before pressing, and the red brocken line is the shape after pressing.

Figure 16 shows comparison of inert explosive shaped body between experiment and simulation results. The shape of the experiment result and the shape of the analysis result are almost the same in the width and height of the shaped body.

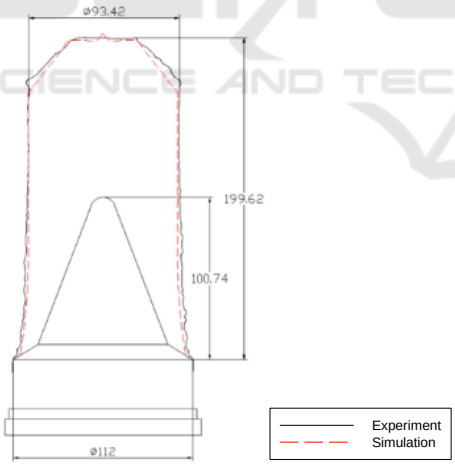

Figure 16: Comparison of inert explosive shaped body between experiment and simulation results.

5 CONCLUSIONS

The results of the double action pressing test and analysis, in the case of the Shima-Oyane yield model showed the results to be almost the same degree of test results and analysis results. The results of the isostatic pressing test and analysis, yield model for test and analysis results showed little difference compared to the height of the molding. Prediction of densification behaviour for inert explosive and the size of the final shape were obtained.

REFERENCES

Lewis RW, Jinka AGK, Gethin DT., 1993. Computer-aided simulation of metal powder die compaction processes. *Powder Metallurgy International*.

Gethin DT, Tran VD, Lewis RW, Ariffin AK., 1994. An investigation of powder compaction process. *International Journal of Powder Metallurgy*.

Kuhn HA, Downey CL., 1971. Deformation characteristics and plasticity theory of sintered powder material. International Journal of Powder Metallurgy.

Shima S, Oyane M., 1976. Plasticity theory for porous metals. *International Journal of Mechanical Science*.

Doraivelu SM, Gelgel HL, Gunasekera JS, Malas JC, Morgan JT., 1984. A new yield function for compressible P/M materials. *International Journal of Mechanical Science*.

Fleck NA, Huhn LT, McMeeking RM., 1992. Yielding of metal powder bonded by isolated contacts. *Journal of the Mechanics and Physics of Solids*.

Kwon YS, Lee LT, Kin KT., 1997. Analysis for cold die compaction of stainless steel powder. *ASME Journal of Engineering Materials and Technology*.

Watson TJ, Wert JA., 1993. On the development an application of constitutive relations for metallic powders. *Metallurgical Transaction.*